ORIGINAL PAPER

Impact of physical parameterization schemes on numerical simulation of super cyclone Gonu

Medha Deshpande · S. Pattnaik · P. S. Salvekar

Abstract   The objective of this study is to investigate in detail the sensitivity of cumulus, planetary boundary layer and explicit cloud microphysics parameterization schemes on intensity and track forecast of super cyclone Gonu (2007) using the Pennsylvania State University-National Center for Atmospheric Research Fifth-Generation Mesoscale Model (MM5). Three sets of sensitivity experiments (totally 11 experiments) are conducted to examine the impact of each of the aforementioned parameterization schemes on the storm's track and intensity forecast. Convective parameterization schemes (CPS) include Grell (Gr), Betts–Miller (BM) and updated Kain–Fritsch (KF2); planetary boundary layer (PBL) schemes include Burk–Thompson (BT), Eta Mellor–Yamada (MY) and the Medium-Range Forecast (MRF); and cloud microphysics parameterization schemes (MPS) comprise Warm Rain (WR), Simple Ice (SI), Mixed Phase (MP), Goddard Graupel (GG), Reisner Graupel (RG) and Schultz (Sc). The model configuration for CPS and PBL experiments includes two nested domains (90- and 30-km resolution), and for MPS experiments includes three nested domains (90-, 30- and 10-km grid resolution). It is found that the forecast track and intensity of the cyclone are most sensitive to CPS compared to other physical parameterization schemes (i.e., PBL and MPS). The simulated cyclone with Gr scheme has the least forecast track error, and KF2 scheme has highest intensity. From the results, influence of cumulus convection on steering flow of the cyclone is evident. It appears that combined effect of midlatitude trough interaction, strength of the anticyclone and intensity of the storm in each of these model forecasts are responsible for the differences in respective track forecast of the cyclone. The PBL group of experiments has less influence on the track forecast of the cyclone compared to CPS. However, we do note a considerable variation in intensity forecast due to variations in PBL schemes. The MY scheme produced reasonably better forecast within the group with a sustained warm core and better surface wind fields. Finally, results from MPS set of experiments demonstrate that explicit moisture schemes have profound impact on cyclone intensity and moderate impact on cyclone track forecast. The storm produced from WR scheme is the most

M. Deshpande (✉) · S. Pattnaik · P. S. Salvekar
Indian Institute of Tropical Meteorology, Dr. Homi Bhabha Road, Pashan, Pune,
Maharashtra 411 008, India
e-mail: medha_d@tropmet.res.in

intensive in the group and closer to the observed strength. The possible reason attributed for this intensification is the combined effect of reduction in cooling tendencies within the storm core due to the absence of melting process and reduction of water loading in the model due to absence of frozen hydrometeors in the WR scheme. We also note a good correlation between evolution of frozen condensate and storm intensification rate among these experiments. It appears that the Sc scheme has some systematic bias and because of that we note a substantial reduction in the rain water formation in the simulated storm when compared to others within the group. In general, it is noted that all the sensitivity experiments have a tendency to unrealistically intensify the storm at the later part of the integration phase.

1 Introduction

Accurate forecast of track and intensity of a tropical cyclone (TC) with a sufficient lead time is essential for disaster mitigation. Numerical models based on fundamental dynamics and well-defined physical processes provide a useful tool for understanding and predicting TC. For accurate forecast of TCs, it is essential that numerical models must incorporate realistic representation of important physical and dynamical processes, those play principal role in determining its genesis, intensification and movement. Anthes (1982) discussed that the physical processes such as cumulus convection, surface fluxes of heat, moisture and momentum and vertical mixing in the planetary boundary layer (PBL) and radiative heating and cooling play an important role in the genesis of tropical cyclones. Frank (1983) illustrated the role of precipitating cumulus clouds in release of latent heat of condensation and its involvement in freezing and melting phase changes in a region of conditional instability. This energy is crucial to the formation and maintenance of the tropical cyclones (Prater and Evans 2002). The degree to which convection moistens the atmosphere is strongly governed by the microphysical characteristics of clouds, which determine how much of the convective water flux is returned to the surface as precipitation and how much to be used to humidify the atmosphere. The exchange of energy at the ocean–atmosphere interface and its supply through the planetary boundary layer (PBL) to the free atmosphere in terms of surface fluxes of latent and sensible heat play an important role in the development, maintenance and intensification of tropical cyclones (Bayers 1944). Emanuel (1986) and Rotunno and Emanuel (1987) showed that the hurricanes can develop and maintain as a result of energy derived from the surface fluxes of latent and sensible heat even if there is no initial convective potential energy in the environment. The scales of all these physical processes are too small to be resolved by numerical models and hence needs to be parameterized in terms of variables defined at the grid points. Willoughby et al. (1984) and Lord et al. (1984) showed the potential sensitivity of simulated tropical cyclone structure and intensity to the cloud microphysics parameterization in a two-dimensional nonhydrostatic model. Their results imply that the structure, intensification and final intensity of a simulated tropical cyclone might be sensitive to the details of the cloud microphysics parameterization used in the numerical models. Puri and Miller (1990) studied the sensitivity of cumulus parameterization using ECMWF analysis-forecast system for four tropical cyclones during the Australian Monsoon Experiment period. Two CPSs were compared, namely, the Kuo scheme (1965) and the Betts–Miller (BM, Betts

1986; Betts and Miller 1986) scheme and concluded that BM scheme has considerable sensitivity in generating more intense cyclonic systems. Braun and Tao (2000) integrated MM5 model with a higher horizontal resolution of 4 km to investigate the sensitivity of planetary boundary layer parameterizations for hurricane Bob-1991. They reported that Burk–Thompson (Burk and Thompson 1989) and Bulk aerodynamic schemes (Deardorff 1972) of PBL produced the strongest tropical cyclone whereas the Medium-Range Forecast (MRF) model PBL (Hong and Pan 1996) scheme produced the weakest storm. Davis and Bosart (2001, 2002) simulated the genesis of hurricane Diana-1984 using MM5 and reported that model physics plays more crucial role during the transition from marginal storm to hurricane strength than during transition from mesoscale vortex to marginal storm strength. Prater and Evans (2002), while simulating hurricane Irene-1999 with BM and Kain–Fritsch (Kain and Fritsch 1993) schemes, have noted that the KF scheme reproduces the track of Irene more accurately. The two parameterizations produce different characteristic vertical warming profiles; the differences in warming are related to the structural differences in the simulated storm, affecting the hurricane response to its environment. Wang (2002) examined the sensitivity of tropical cyclone development to cloud microphysics schemes and reported that the intensification rate and final intensity are not sensible to cloud microphysics but only produce differences in the cloud structure. Yang and Ching (2005) simulated typhoon Toraji-2001 and studied the sensitivity to different parameterization schemes. They reported that Grell convection scheme (Grell 1993), Medium-Range Forecast (MRF) model PBL and Goddard Graupel (Tao and Simpson 1993) cloud microphysics scheme give the best track and intensity that most resemble with the observations. Pattnaik and Krishnamurti (2007) investigated the impact of cloud microphysical processes on hurricane intensity using 4-km resolution simulations. They found that inter-conversion processes, such as melting and evaporation among the hydrometeors and associated feedback mechanism, significantly modulate the intensity of the hurricane.

In the North Indian Ocean basin, the case of Orissa Super Cyclone (1999) in the Bay of Bengal has been studied by many researchers using MM5. Mandal and Mohanty (2006) found that Grell cumulus parameterization scheme with MRF PBL scheme and NCAR community climate model (CCM2, Briegleb 1992; Kiehl et al. 1994) radiation parameterization scheme provides the optimal combination of the physical processes parameterization schemes (the central sea level pressure of 963 hPa against 912 hPa observed one). Trivedi et al. (2006) reported that with a single domain of 50-km resolution, Kain–Fritsch, MRF and Simple Ice (SI, Dudhia 1989) is the better combination of model physics compared with other physics combination but the simulated intensity is underestimated (the central sea level pressure of 966 hPa). The extensive sensitivity study by Rao and Prasad (2006, 2007) reported the minimum track error with the combination of updated Kain–Fritsch (KF2, Kain 2004), Mellor–Yamada (MY, Mellor and Yamada 1982) and Mixed Phase (MP, Reisner et al. 1998), for which the simulated minimum pressure was 930 hPa. Srinivas et al. (2007) studied the sensitivity to the PBL and convective parameterization schemes to the numerical simulation of Andhra Severe Cyclone (2003) in the Bay of Bengal. Their result indicates that while the boundary layer processes play a significant role in determining both the intensity and movement, the convective processes especially control the movement of the model storm. The combination of MY PBL and KF2 convection scheme gives the most intensive storm and the MRF PBL with KF2 convection scheme produces the best simulation in terms of intensity and track compared to observations. Using MM5, Mandal et al. (2004) studied the impact of various physical parameterization schemes on the prediction of two tropical cyclones formed during

November 1995 over the Bay of Bengal and found that the combination of MRF PBL scheme with Grell cumulus scheme performed better than other combinations. Though a number of parameterization schemes are developed for implicit treatment of these important physical processes, theses schemes have certain limitations (Frank 1983; Molinari and Dudek 1992; Emanuel and Raymond 1993; Zhang et al. 1994; Kuo et al. 1997) and are regime specific. Thus, it is desirable to evaluate and highlight the suitability of individual parameterization schemes and their combinations for accurate forecast of intensity and track of the cyclones over various regions and seasons.

The objective of this study is not only to carryout the sensitivity tests and obtain the optimal combination of physical parameterization schemes for improving track and intensity forecast of the storm but also to illustrate possible mechanisms responsible for these results. The super cyclone Gonu (2007) in North Indian Ocean over the Arabian Sea during monsoon season is considered for this study. In the next section, the brief description of the super cyclone Gonu obtained from India Meteorology Department report (IMD 2008) is given followed by description of the model and designing of numerical experiments and data used. The results and discussion are presented in Sect. 4 and concluding comments are illustrated in Sect. 5.

2 Brief description of super cyclone Gonu (2007)

The Super Cyclonic Storm Gonu 2007 was the strongest tropical cyclone on record in the Arabian Sea (IMD 2008). Intense cyclones like Gonu have been extremely rare over the Arabian Sea, as most storms in this area tend to be small and dissipate quickly. A low pressure area with persistence convection developed over east central Arabian Sea in association with the prevailing surge in monsoon flow. During this period, there was favorable upper-level environment and warm sea with sea surface temperature of the order of $27-29°C$ over the Arabian Sea. As a result a system concentrated into a depression and lay centered over east central Arabian Sea near 15°N and 68.5°E at 1800 UTC of June 1. Initially, the system moved in the westward direction and concentrated into deep depression at 0300 UTC of June 2 and into cyclonic storm "GONU" at 0900 UTC and lay centered over 15°N and 67°E. Moving in a northwest direction, it further intensified into a severe cyclonic storm at 0000 UTC of June 3 and lay centered over 15.5°N and 66.5°E. The eye of the system was first visible at 0600 UTC of June 3 from KALPANA satellite imagery. At this time, the ridge in upper air was located at about 16°N over the storm region. Moving in northwest direction it again intensified into a very severe cyclonic storm at 1800 UTC of 3 June. The eye was raged within the central dense overcast (CDO). The system further intensified into a super cyclonic storm and lay centered at 1500 UTC of June 4 and lay centered over 20°N and 64°E, with lowest estimated central pressure of 920 hPa and maximum sustained surface winds of 127 knots (65.3 m/s).

The system maintained super cyclonic storm intensity for a short period and weakened into a very severe cyclonic storm at 2100 UTC of June 4 due to entrainment of dry and cold air and cold sea water over the region. Moving in the west-northwestward direction, it crossed Oman coast as a very severe cyclonic storm between 0300 and 0400 UTC of 6 June. The system then emerged into the Gulf of Oman, moved in a north-northwestward direction and made second landfall over Iran coast near 25.5°N and 58.5°E between 0300 and 0400 UTC of June 7, 2007, as a cyclonic storm. Moving in the same direction, it weakened gradually, and it was seen as a well marked low pressure area over Iran and neighborhood on June 8, 2007. The cyclone caused about $4.2 billion in damage (2007

USD), 50 deaths and 20,000 people were affected in Oman, where the cyclone was considered the nations worst natural disaster. Gonu dropped heavy rainfall near the eastern coastline, reaching up to 610 mm (24 inches), which caused flooding and heavy damage. In Iran, the cyclone caused 28 deaths and $215 million in damage (2007 USD).

3 Numerical model and experiment design

The Penn State/NCAR MM5 (version 3.7) is used to carry out the sensitivity experiments for this study. The MM5 is a nonhydrostatic model with a terrain following sigma vertical coordinate system. Detailed description of MM5 is given by Grell et al. (1994). The model consists of a number of physical parameterization schemes, providing an opportunity to carry out various sensitivity studies. The sensitivity experiments with different convective parameterization schemes (CPS) include Grell (Grell 1993), Betts–Miller (Betts and Miller 1986) and updated Kain–Fritsch (Kain 2004). Similarly sensitivity experiments with different planetary boundary layer parameterization schemes (PBL) include Burk–Thompson (Burk and Thompson 1989), Eta Mellor–Yamada (Mellor and Yamada 1982) and the NCEP Medium-Range Forecast model PBL (Hong and Pan 1996). In addition, six cloud microphysical schemes including Hsie's Warm Rain (Kessler 1969), Dudhia's Simple Ice (Dudhia 1989), Reisner's Mixed Phase (Reisner et al. 1998), NASA/Goddard microphysics with hail/graupel (Tao and Simpson 1993; modified by Braun and Tao 2000), Reisner's Mixed Phase with graupel (Reisner 2, Reisner et al. 1998; modified by Thompson et al. 2004) and Schultz (Schultz 1995) Mixed Phase with graupel are chosen to for carrying out sensitivity experiments with microphysical parameterization schemes (MPS).

For all experiments, NCAR community climate model (CCM2) (Briegleb 1992; Kiehl et al. 1994) radiation parameterization scheme is used. It is well documented that these parameterizations schemes continuously interact with each other throughout the model integration duration. The cumulus parameterization modifies the cloud water/vapor content through detrainment, which in turn affects the cloud microphysics. The microphysics parameterization determines the ice and water content in the atmosphere and this affects the radiation. The radiation and PBL parameterizations interact through the surface fluxes given by the five-layer soil scheme. However, here, we would like underscore the point that for each set of experiments (Table 1) all model configurations (i.e., resolution, initial condition, model physics, dynamics) are same except specific parameterization scheme is changed in all the domains for each sensitivity simulation experiment. This has been done with an objective to exclusively attribute the sensitivity of specific parameterization scheme on the model forecast results. Table 1 lists the combination of physical parameterization schemes of all the numerical experiments carried out in this study.

For CPS and PBL experiments, the model is configured in a two-way nested fashion having two domains with 90-, 30-km grid resolutions, whereas for MPS experiments, triply nested domains (three domains) with grid resolution of 90, 30 and 10 km are used. This is to note that cumulus parameterization scheme is used for MPS experiments (including the inner most domain) because of the coarser horizontal resolution (i.e., 10 km). All model domains have 23 vertical unequal σ levels with higher resolution in the planetary boundary layer. Figure 1 shows the multiple nest area coverage of the 3 domains (hereafter D1, D2 and D3), centered over 15°N and 65°E. Domain D3 covers entire track of the observed cyclone during the integration phase. Middle domain D2 covers the Arabian Sea region, whereas outer domain D1 covers large extended region on the four sides of the region of interest so as to simulate the large scale atmospheric flow during onset phase of the

Table 1 Physical parameterization scheme used in each numerical experiment

Experiment	Cumulus	PBL scheme	Microphysics
CPS: Test of cumulus parameterization (two domains, D1 and D2)			
Gr*	Grell	Eta Mellor–Yamada	Mixed Phase
BM	Betts–Miller	Eta Mellor–Yamada	Mixed Phase
KF2	Kain–Fritsch 2	Eta Mellor–Yamada	Mixed Phase
PBL: Test of PBL parameterization (two domains, D1 and D2)			
BT	Grell	Burk–Thompson	Mixed Phase
MY*	Grell	Eta Mellor–Yamada	Mixed Phase
MRF	Grell	NCEP MRF	Mixed Phase
MPS: Test of microphysics parameterization (three domains, D1, D2 and D3)			
WR	Grell	Eta Mellor–Yamada	Warm Rain
SI	Grell	Eta Mellor–Yamada	Simple Ice
MP	Grell	Eta Mellor–Yamada	Mixed Phase
GG	Grell	Eta Mellor–Yamada	Goddard Graupel
RG	Grell	Eta Mellor–Yamada	Reisner Graupel
Sc	Grell	Eta Mellor–Yamada	Schultz

* These two experiments are identical

D1, Domain 1; D2, Domain 2; D3, Domain 3 (90-, 30- and 10-km grid resolution, respectively, Fig. 1)

monsoon. The initial and boundary conditions for the three model domains are obtained from NCEP's final analysis (FNL) data sets with $1° \times 1$ horizontal resolution. The time varying lateral boundary conditions are obtained at every 12 h interval during the entire simulation period (i.e., from 1200 UTC June 2, 2007, to 0000 UTC June 6, 2007). The model is integrated in a two-way interactive fashion. All model results are from 30 km domain unless it is mentioned otherwise.

4 Results and discussions

In this study, totally 11 experiments were conducted to investigate the sensitivity of simulated track, central sea level pressure (CSLP) and maximum wind speed (MWS) at lowest model level (0.995 σ level) of the tropical cyclone Gonu-2007 to three kinds of physical parameterization schemes (i.e., cumulus, planetary boundary layer and microphysics).

4.1 Sensitivity to cumulus parameterization schemes

In this group, three experiments are carried out with the variation only in the cumulus parameterization schemes. The convection schemes used are Grell (Gr), Betts–Miller (BM) and updated Kain–Fritsch (KF2) in combination with Eta Mellor–Yamada (MY) scheme for PBL and Mixed Phase (MP) scheme for cloud microphysics.

Figure 2a–d shows the model-simulated tracks, forecast track errors and intensity in terms of CSLP and MWS of Gonu for the experiments obtained from aforementioned convection schemes along with observed best fit track and intensity obtained from Indian Meteorological Department (IMD), respectively. The forecast tracks (Fig. 2a) indicate
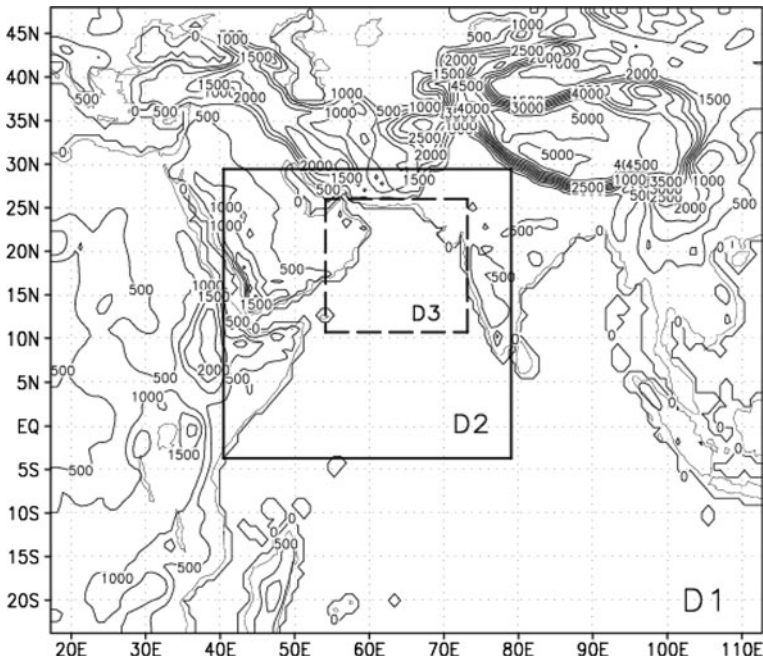
Fig. 1 Model domains with 90-km (D1), 30-km (D2) and 10-km (D3) resolution. Contour shows terrain height in meters

strong deviations from the observation. The observed movement of the storm is almost in the north-westward direction throughout the integration period. The track obtained from BM and KF2 experiments show northward movement initially and then recurved in north-eastward direction after 48 h of integration. It appears that translational speed of the storm is slower in the case of BM and faster in case of KF2 compared to observation. Throughout the integration phase, Gr storm moves closely to the observed track (i.e., IMD) but with much slower forward speed. This feature prohibits the landfall of the storm.

Figure 2b displays the time variation of track error of the storm in kilometers. It is clear that throughout the integration phase Gr carries the least amount of error. In general after 30 h of model integration there is an increasing trend in magnitude of track forecast errors in all the simulations. The average track error is 161 km, 382 km and 381 km for Gr, BM and KF2, respectively. The time variation (6 h) of CSLP in hPa and MWS in m/s are displayed in Fig. 2c and d, respectively, for this group of experiments. The results show that CSLPs at the most intense phase of storm (i.e., 54th h of integration) obtained from the Gr, BM and KF2 experiments are 980, 979 and 960 hPa, respectively. Correspondingly the storm's MWS are 30, 28 and 38 ms^{-1}, respectively. At this most intense phase of the storm, the observed CSLP and maximum surface wind recorded are 920 hPa and 65.3 ms^{-1}, respectively. The results indicate that the intensity of KF2 storm is somewhat close to that of the observed intensity (i.e., IMD) but in general all the forecasts obtained from these experiments have largely underestimated storm intensity. However, considering track and intensity both in view forecast obtained from Gr scheme is relatively better in the group.

These results clearly demonstrated the profound sensitivity of cyclone's track and intensity forecast to the variations in cumulus parameterization schemes. Now we would
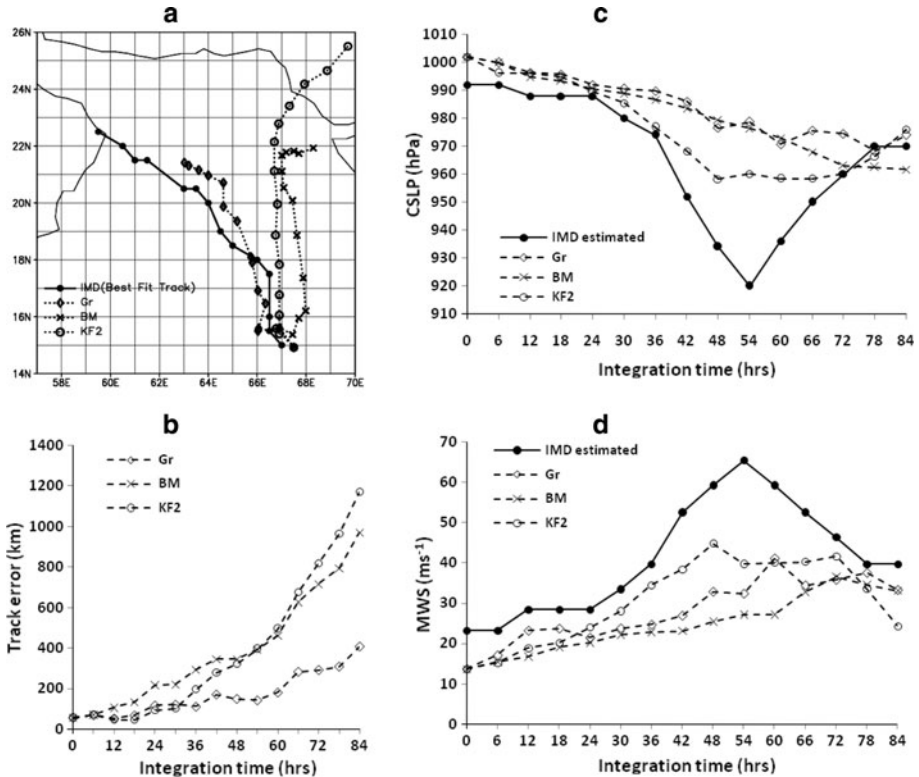
Fig. 2 a Model-simulated tracks, **b** forecast track error, **c** time series plot of central sea level pressure (CSLP) in hPa and **d** time series plot of maximum wind speed (MWS) at the lowest model level for the experiments with different convection parameterization schemes (CPS) obtained from the results of D2 along with IMD best fit track, CSLP and MWS data. The total duration of model integration is 84 h, with integration started at 1200 UTC June 2, 2007. The time interval of track and intensity is 6 h

like to discuss some of the possible causes for these results. Figure 3a–l represents 500 hPa geopotential heights in meters (shaded) and wind direction (vectors) for each of these experiments in the outermost mesh (90 km) and from the NCEP FNL reanalysis data (1° × 1°). The first column (a–d), second column (e–h), third column (i–l) and fourth column (m–p) represent NCEP, Gr, BM and KF2, respectively. First, second, third and fourth row in Fig. 3 represent geophysical parameters at 24, 48, 72 and 84 forecast hours, respectively. Analyzing the later part of the forecast (i.e., 72 h onwards), it appears that strength of the eastward moving midlatitude trough to the north of the storm considerably influenced the storm in KF2 and BM experiments and facilitating their respective progress in north and north easterly direction. We also like to highlight that an intense storm such as KF2 with a stronger trough interaction perhaps resulted in a much faster translational speed of the storm than others. The combined impact of minimal trough interaction and stronger southerly surge of winds at the mid-level appears to be facilitating the north-westward movement of the storm in NCEP and Gr. In addition to this, it is evident that the horizontal extent and strength of anticyclone formed west of the forecast tracks prohibits the west-ward progress of KF2 and BM storms. However, the strength of the anticyclone formed in Gr scheme is moderately weaker to facilitate the westward propagation of the storm. As far
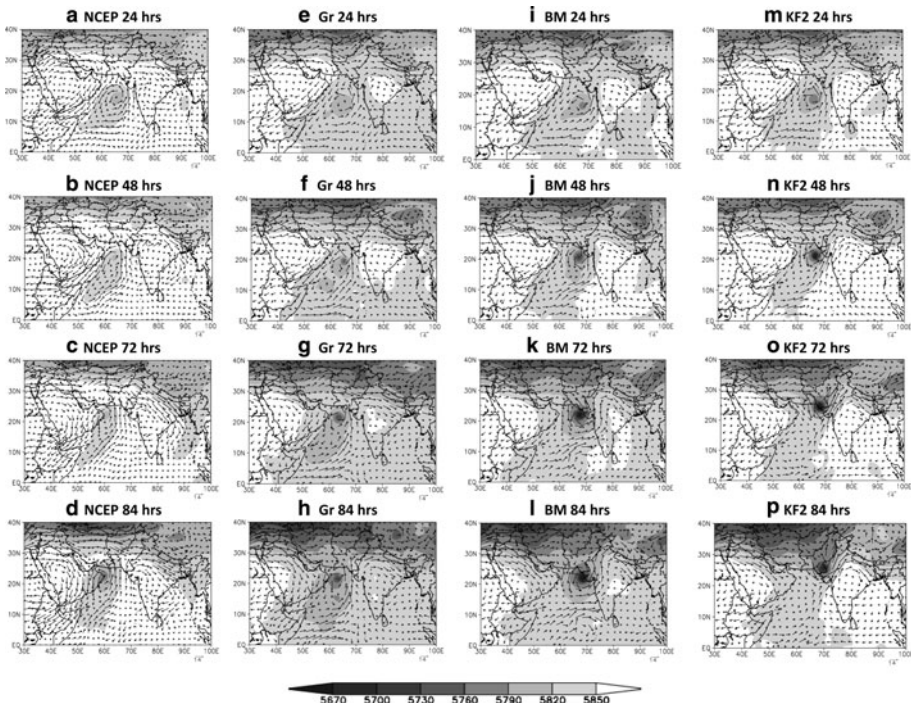
Fig. 3 a–l Geopotential height in meters (*shaded*) and wind direction (*vectors*) at 500 hPa for CPS experiments in the outermost mesh (D1 90 km) at 24, 48, 72 and 84 forecast hours

as forward speed of Gr is concerned, results indicate that joint influence of weak trough interaction, anticyclone to the west and a less intensity of the storm might be responsible for this slow propagation speed. These results clearly demonstrate the robust impact of cumulus parameterization on the large scale environment.

Figure 4a–i displays the day 1, day 2 and day 3 accumulated convective rainfall (i.e., sub-grid scale) in mm for 24 h duration for each of the experiments. It is clear that BM and KF2 are producing a lot more sub-grid scale precipitation compared to Gr. This large amount of precipitation releases significant amount of latent heat and this provides a positive feedback to the eyewall buoyancy and reducing pressure thus facilitates inflow and intensification of the storm. Underestimation of grid scale precipitation in Gr Scheme attributed to its systematic limitations in removing instability efficiently from the model. We have also shown 24-h-averaged vertical cross section of potential vorticity (PV) between 24 h and 48 h of integration across the eyewall of the respective storm core in Fig. 5a–c. It is well known that PV is a good indicator for latent heat release, as latent heating impacts its two principal components (i.e., absolute vorticity and static stability). Therefore, rate of generation and destruction of potential vorticity also largely depends upon magnitude and gradient of latent heating. Figure 5 elucidates the area and magnitude of latent heat release from the vertical structure of upper tropospheric PV in the storm core. We note that KF2 storm produced significantly higher latent heat compared to BM and Gr scheme, therefore becoming the most intense storm. We would also like to underscore the point that this immense release of heat in respective stimulations might have influenced the necessary adjustments in large scale fields that directly affect the track forecast of the
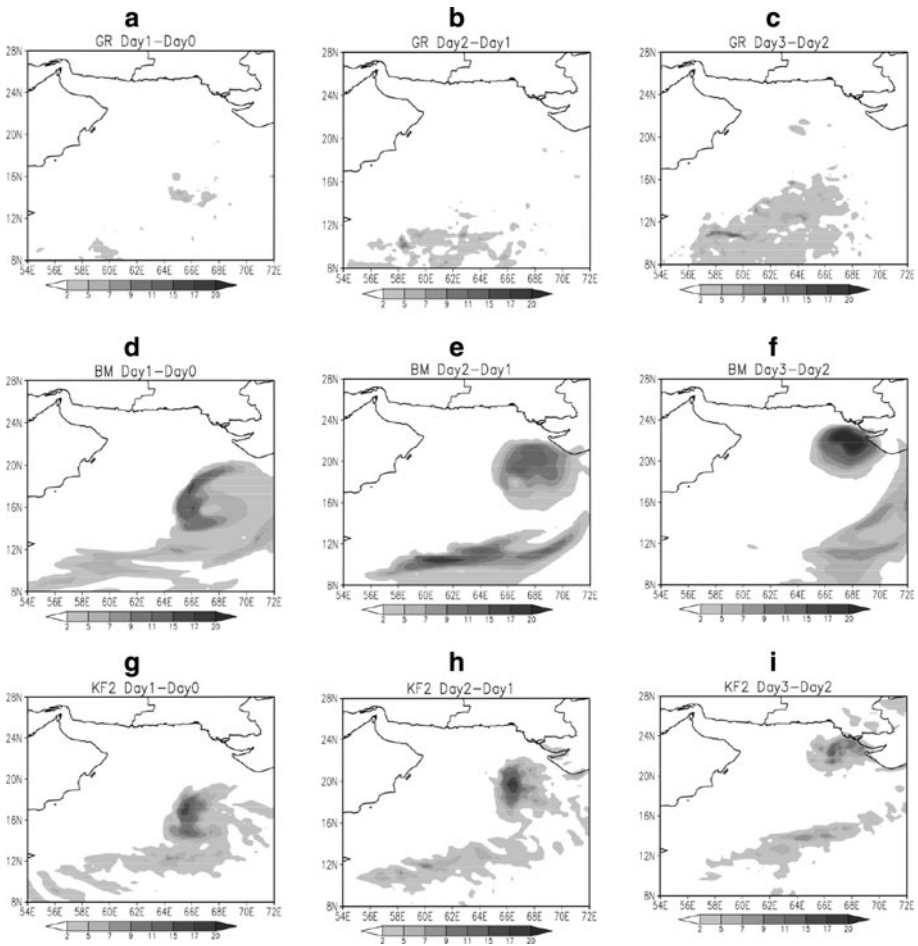
Fig. 4 **a–i** Convective rainfall (mm) accumulated in 24 h for day 1, day 2 and day 3 for CPS experiments in D2

storm. From these results, it is evident that there are combination of important dynamical factors working together to determine the path of the forecast track and propagation speed of the storm. They are the intensity of the cyclone, strength of the anticyclone to the west of the storm, southerly surge of wind and the strength of the prevailing trough to the north of the storm.

4.2 Sensitivity to PBL parameterization schemes

This set of experiments comprises three experiments with variations only in planetary boundary layer (PBL) parameterization scheme keeping the rest of the model configuration unchanged. The PBL schemes considered here are Burk–Thompson (BT), Mellor–Yamada (MY) and Medium-Range Forecast (MRF). Based on results in the previous section Gr, MP and CCM2 schemes are used for cumulus, explicit moisture and radiation parameterizations, respectively, in the model along with the aforementioned PBL schemes.

Fig. 5 a–c Vertical cross section of 24-h-averaged potential vorticity between 24 h and 48 h of integration across the eyewall of the storm core for CPS experiments
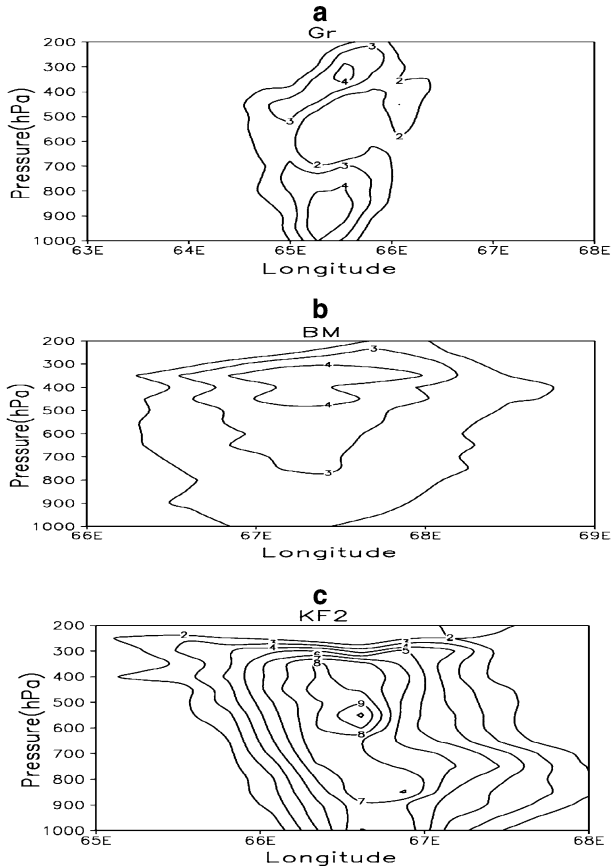
The forecast tracks and intensity for these experiments along with IMD observations are presented in Fig. 6. Figure 6a, b represents forecast track and forecast track errors in kilometers, respectively. Drastic variations in track forecast are not noticed up to 36 h (maximum difference of track error is roughly 25 km) from these results. Significant increases in forecast track error are found after 42 h, with MRF having the largest track errors (greater than 400 km at 72 h of forecast). However, we do note more westward bias in the forecast track of BT compared to others. The average track error is 168, 167 and 222 km for BT, MY and MRF, respectively. The forward speeds of the simulated storms are significantly underestimated when compared to the observation; therefore, none of the forecast tracks made a landfall during the model integration period. We also note that the forward speed of the MY storm is relatively better in the group. The time variations in the intensity of the storm for this group of experiments are shown in Fig. 6c and d in terms of CSLP and MWS, respectively. It shows neither of the storm's intensity matches with the observed strength of the storm (i.e., 920 hPa) nor any of these storms is able to replicate the rapid intensification phase of the storm. However, looking at the intensity, track error and translational speed throughout the integration time duration, it appears that the forecast produced from MY scheme is reasonably better compared to MRF and BT. It also suggests that MY scheme not only produced but also sustained the high intensity of the storm throughout the forecast duration.
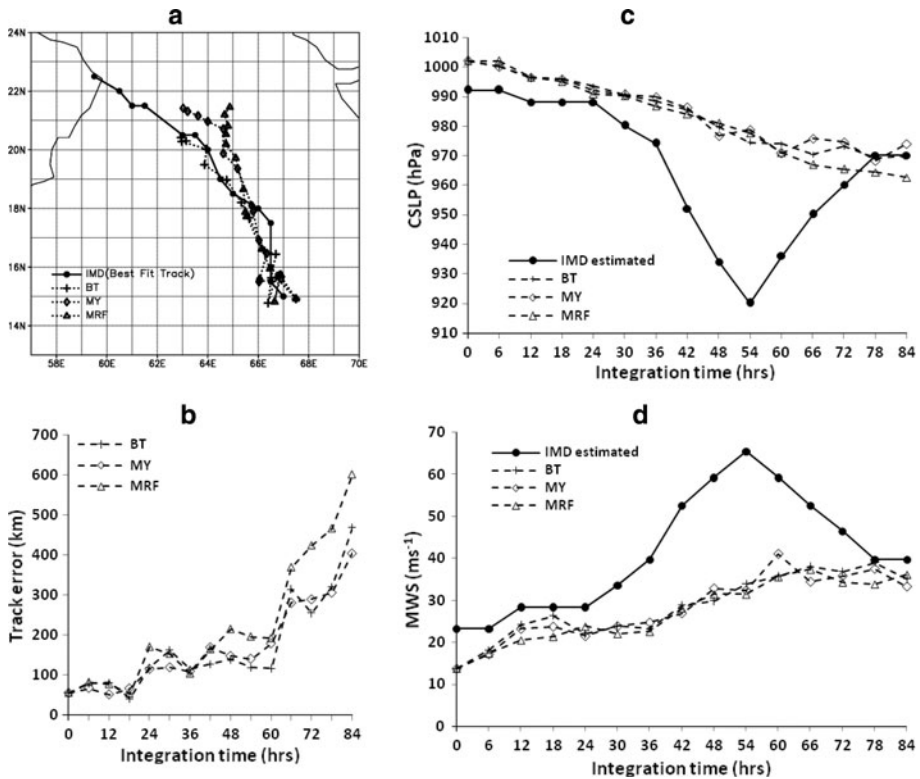
Fig. 6 a–d Same as Fig. 2 but for the experiments with different planetary boundary layer (PBL) parameterization schemes

To elucidate possible causes of these results, we have presented snapshot of equivalent potential temperature deviation (K) and time series of surface net heat flux (SNHF) in W/m^2 in Fig. 7. Figure 7a–c represents layer-averaged deviation of equivalent potential temperature at the most intense phase of the storm (i.e., 54th forecast hour). The equivalent potential temperature is well recognized as a good indicator for analyzing tropical cyclone intensity. This parameter represents the combination of both heat and moisture in a single variable (Betts and Simpson 1987). The results in Fig. 7a–c suggest that maximum warming for MY and BT schemes (20 K) is twice as high as MRF scheme (10 K). In addition to the equivalent potential temperature, surface net heat flux (SNHF) in general and latent heat flux (LHF) in particular are considered as principal source for energy of hurricane intensification (Ooyama 1969; Riehl 1954; Palmén and Riehl 1957). These surface fluxes (i.e., sensible heat flux and latent heat flux) maintain the cyclone thermodynamically by transporting heat and moisture from ocean surface into the storm. So, Fig. 7d displays the area-averaged SNHF (W/m^2) of these storms during the entire integration time period. Here, the SNHF is the sum of surface latent heat flux (SLHF) and surface sensible heat flux (SSHF). It is noted that the characteristic variations in SNHF are well in correspondence to the cyclone intensity variations except for MRF. It is interesting to note that even though the quantitative magnitude of SNHF in MRF scheme is almost twice larger than that of BT and MY scheme (Fig. 7d); MRF storm strength does not correlate well with its magnitude of variations in SNHF. We mainly attribute the cause of
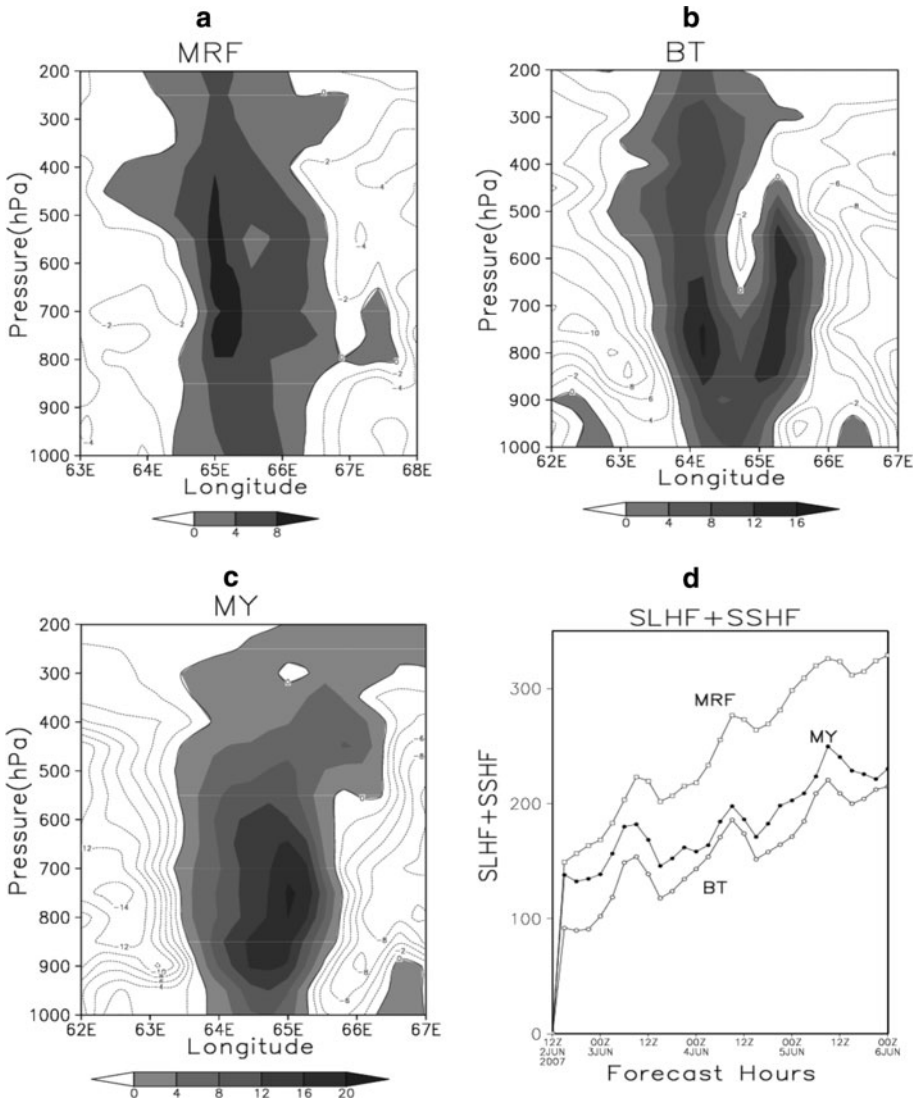
Fig. 7 **a–c** Snapshots of layer-averaged deviation of equivalent potential temperature at the most intense phase of the storm (i.e., 54th forecast hour) and **d** time series of surface net heat flux (SNHF) in Watts/m² for PBL experiments obtained from D2

this inconsistency to the overestimation of surface fluxes tendency in MRF PBL scheme due to large values of eddy exchange coefficient (Liu et al. 2004; Braun and Tao 2000) and intense deep vertical mixing in MRF scheme which dries up the lower PBL leads to an underestimation of the storm surface winds that reduce storm intensity (Braun and Tao 2000). As far as MY and BT schemes are concerned the pattern of storm intensity variations are somewhat replicated in their respective forecasts but magnitude of the storm intensity is far lower than that of observations. Keeping our results in view, it is reasonable to say that MY scheme performed better in the group. We have reached this inference by

considering a combination of factors such as better forecast of track, translational speed and variations in the magnitude of the storm intensity.

4.3 Sensitivity to cloud microphysics parameterization schemes

This group comprises six experiments elucidating the impact of different microphysical parameterization schemes (MPS) on forecast track and intensity of the cyclone. The explicit parameterization schemes are Warm Rain (WR), Simple Ice (SI), Mixed Phase (MP), Goddard graupel (GG), Reisner graupel (RG) and Schultz (Sc). Here, we would like to underscore that these simulations are carried out in a triply nested fashion with horizontal resolutions of 90, 30 and 10 km. Based on previous results Gr, MY and CCM2 have been included as cumulus, planetary boundary layer and radiation parameterization schemes, respectively, for these experiments. All the results discussed here are obtained from the inner most nest of 10-km resolution.

The forecast track and intensity of these experiments are presented in Fig. 8. In general, the track forecasts of these storms (Fig. 8a) do not vary much except eastward biases in the track of Sc and GG experiments. The time variation of forecast tracks errors are displayed in Fig. 8b, which indicates that track error has been increased significantly (>150 km) after 60 h of forecast for all the experiments. Prior to 60 h of forecast GG gives the lowest error most of the time with minimum error of 18 km at 18th forecast hour. During total
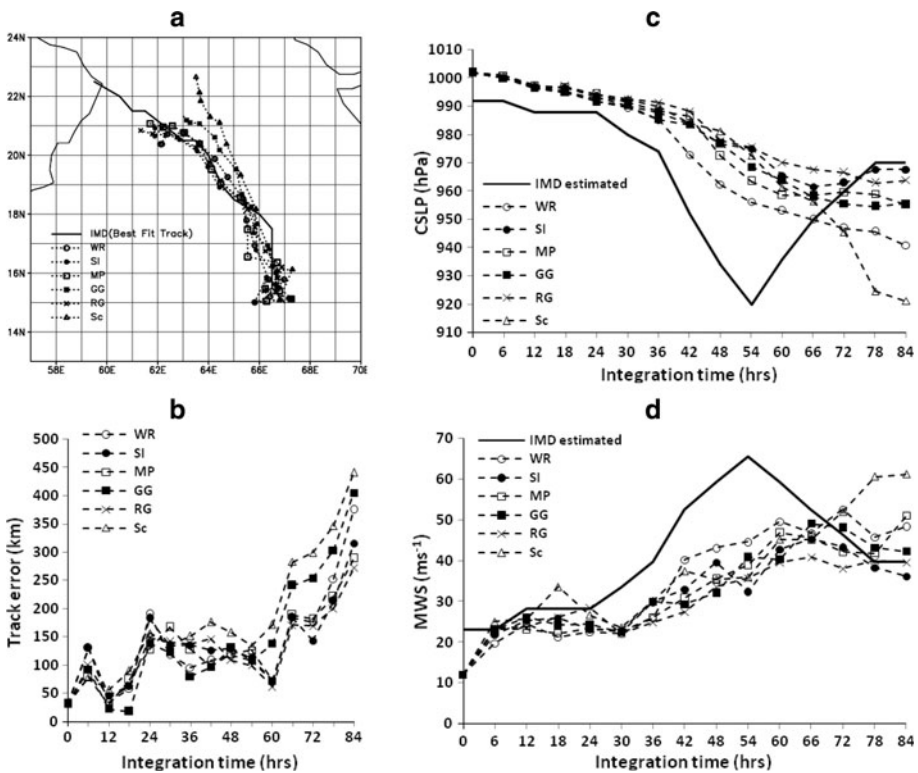

Fig. 8 a–d Same as Fig. 2 but for the experiments with different cloud microphysics parameterization schemes (MPS) obtained from D3

integration period, average track error is 136 km, 134 km, 129 km, 145 km, 126 km and 180 km for WR, SI, MP, GG, RG and Sc, respectively. The forward speeds of the storms obtained from all the experiments are much slower compared to that of the observed. However, we do note an improvement in forward speed of the respective storms compared to previous experiments (i.e., PBL and CPS experiments). Time variations of the storm intensity in terms of CSLP and MWS are displayed in Fig. 8c and d, respectively. If we look between 36 and 66 forecast hours, it is clear that storm rapidly intensified and then slowly loses its strength; it is evident that the WR storm intensity is most close to the observed intensification rate followed by MP and GG. Considering the forecast skills in terms of track and intensity for the storm, it is clear that WR, MP and GG are the best three in the group. Their respective CSLP (hPa units) are 956, 963, 968 and MWS (ms^{-1} units) are 44, 39, 40 at 54 h of forecast (i.e., most intense snapshot of the storm).

Figure 9a–c presents area-averaged vertical profiles of total water loading in g/kg units at 24, 48 and 72 forecast hours. The total water loading includes cloud liquid water (CLW), rain water (RNW), ice (ICE), snow (SNW) and graupel (GRA). It indicates that strongest storm WR has produced large amount of RNW and CLW in the upper troposphere compared to MP and GG. The presence of more liquid in the upper troposphere for WR storm is due to the absence of frozen hydrometeors such as ICE and SNW in the parameterization scheme. It is interesting to note that there is a maximum of liquid hydrometeors (mostly RNW) between 950 and 900 hPa in all MPS experiments except Sc experiment. As the forecast hours increases, we note corresponding increase in magnitudes of frozen condensate at the upper level as well as liquid hydrometeors at the lower level. This indicates that the inter-conversion of hydrometeors is taking place through melting process of frozen hydrometeors and this is mostly contributing to the increase in liquid phase at the lower level. However, this feature is again not noted for Sc experiment. In order to understand further the intriguing nature of the Sc experiment, we have plotted the time series of domain-averaged vertical profiles of frozen (ice + snow + graupel) as well as liquid (rain water + cloud water) hydrometeors for four experiments MP, GG, RG and Sc shown in Fig. 10a–d, respectively (these four schemes have ice phase in it). These figures will supplement our understanding on temporal evolution of hydrometeors throughout the duration of model integration. From these figures, it appears that there is good correlation between amount of frozen hydrometeors at the upper level and storm intensification pattern. However, the most interesting thing, we note is for experiment Sc. From Fig. 10d, it is conspicuous that the formations of liquid phase of hydrometeors (i.e., rain water) are substantially less throughout the forecast duration when compared to other experiments. We also note that between GG and MP experiments, even though both have similar quantity of rain water at the surface, the presence of more frozen hydrometeor concentration in MP perhaps helping the storm to be stronger because of additional condensational heating contribution. In the case of Sc experiment, we noted a much delayed (24 h later than observed) rapid intensification of the storm has happened (Fig. 8c). This is perhaps due to large scale reduction in melting process which leads to reduction in cooling tendencies in the storm core and at the same time gradual accumulation of frozen hydrometeor might lead to more addition of condensational heating and because of this combination storm rapidly flared up after 60 h of forecast and continued its intensification unrealistically afterward. For RG experiment (Fig. 10c), it is clear that in spite of less accumulation of frozen condensate (quantity and distribution) the formation of RNW remains same compared to GG and MP experiments. This indicates that in the RG experiment the cooling tendencies from melting and evaporation process are dominating throughout the model integration duration. This might be resulting in a weaker storm.
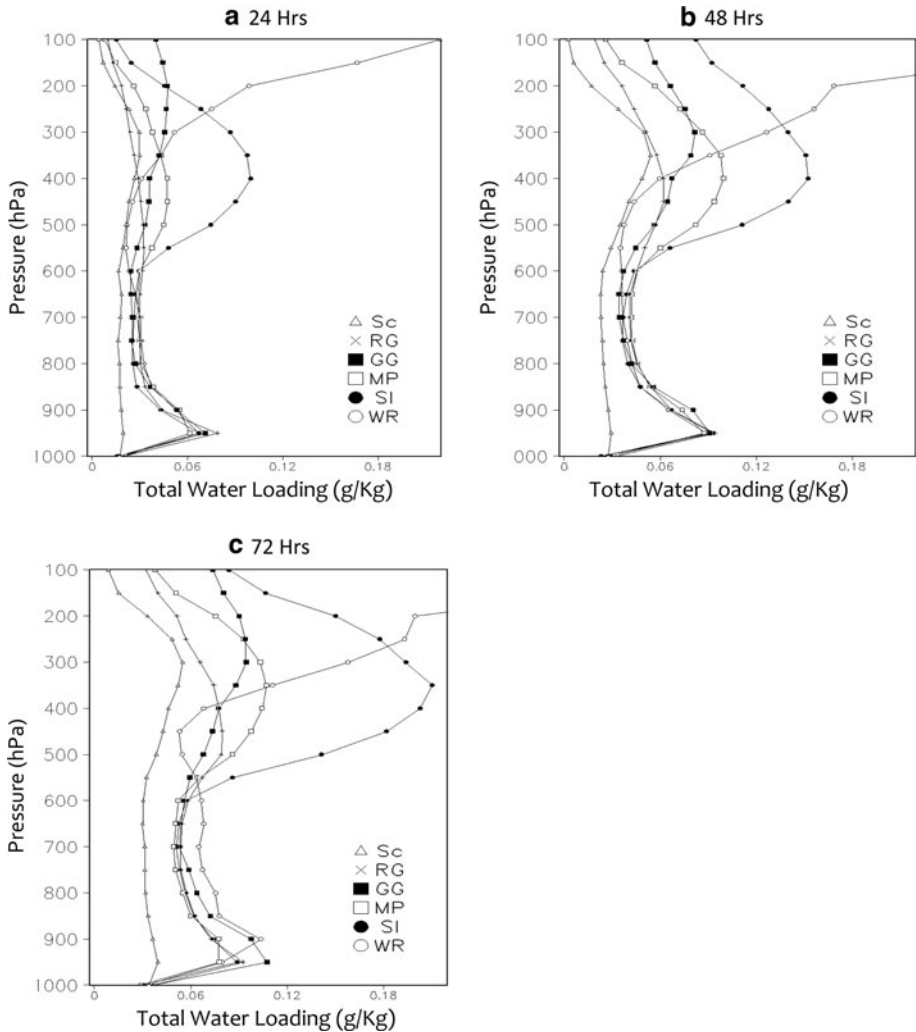
Fig. 9 a–c Domain-averaged vertical profile of integrated frozen and liquid hydrometeors (total water loading) for all MPS experiments for 24, 48 and 72 forecast hours from D3. Units are g/kg

Based on these results, we attribute mainly two reasons for the maximum intensification of the storm in WR experiment. First, due to the absence of physical processes such as melting and evaporation of frozen hydrometeors (i.e., snow, ice and graupel) the cooling tendency within the storm core has been significantly reduced (intense warming in the core, figure not shown). Secondly, the total water loading in WR is lower when compared to MP and GG (Fig. 9a–c). This reduction in water loading for WR further enhance the acceleration of updraft air parcel within the core facilitating influx of more moisture, heat and momentum from the surface and leads its intensification. Overall, it is evident that because of major differences in generation, dissipation and distribution of hydrometeors in each of these explicit moisture schemes, their respective impact on storm intensity, track, precipitation and inner core structures are robust.
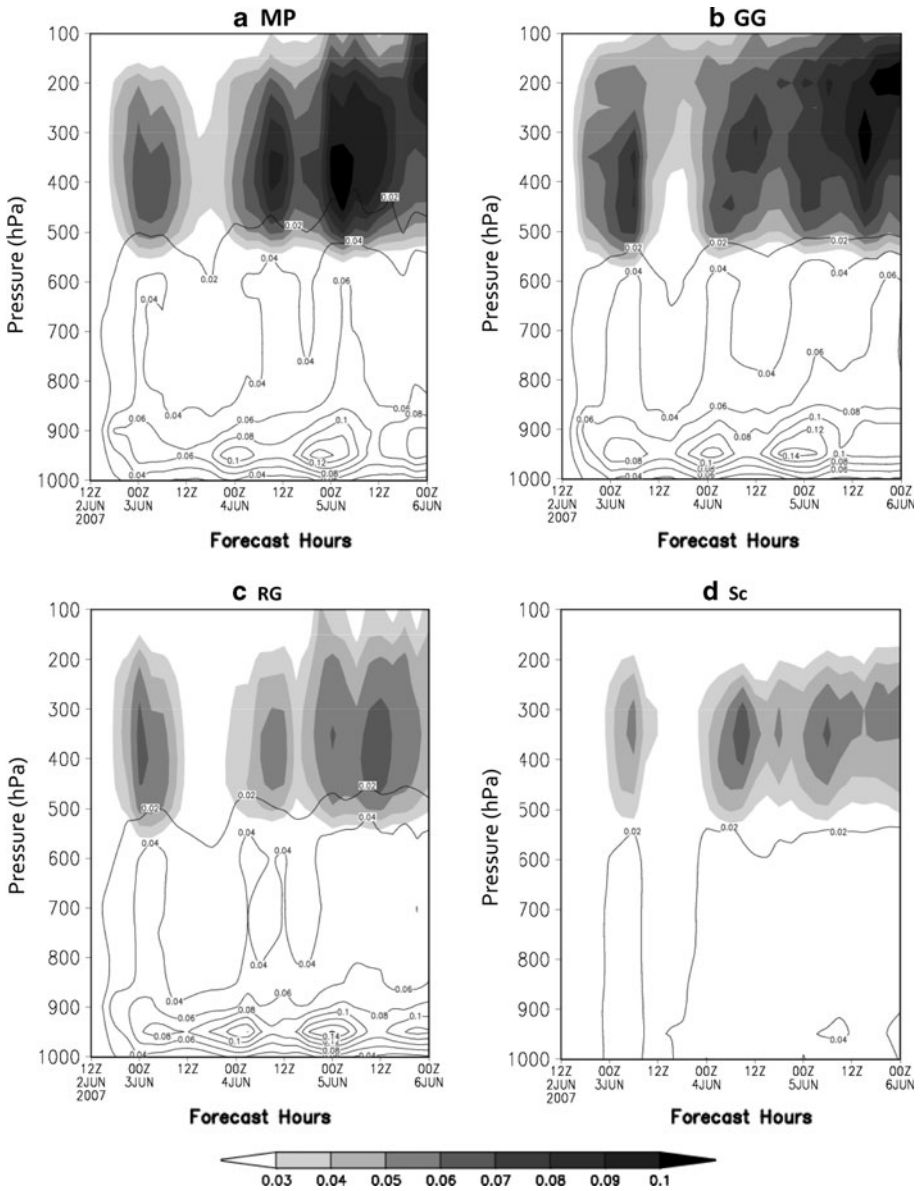
Fig. 10 a–d Domain-averaged evolution of frozen hydrometeors (snow, ice and graupel) in shaded and liquid hydrometeors (rain water and cloud water) in contours for experiment MP, GG, RG and Sc obtained from the D3. The units are g/kg

5 Summary and conclusions

Our result suggests physical parameterizations in MM5 have large sensitivity on intensity and track of cyclone Gonu. Here, an attempt is also being made to elucidate possible mechanisms for this intensity modulation. The cumulus convection experiments (CPS)

results suggest Gr scheme produced the best track and KF2 produced a storm with better intensity. The impact of cumulus convection schemes on large scale environment is well demonstrated from CPS experiments. The influence of midlatitude trough, strength of anticyclone to the west of the storm and intensity of the individual storm appears to be the main factors responsible for steering respective storm tracks obtained from these experiments. There are two other issues we have highlighted in our CPS discussion; they are precipitation and potential vorticity. The quantitative amount and distribution of these two parameters are well correlated to the latent heat release in the storm. We have shown that the intense storm such as BM and KF2 have produced large amount of precipitation and potential vorticity compared to Gr. The quantity of sub-grid scale precipitation is largely underestimated in Gr because of its systematic inefficiency to remove instability from the model.

The results from PBL sensitivity experiments indicate that all the simulated forecast tracks obtained have less track error compared to CPS experiments. The pattern of intensification rate is somewhat reproduced for MY experiment up to 60th forecast hour in the group. However, none of the experiment has achieved the observed strength of the storm. We have investigated the area average of total surface heat fluxes (i.e., latent heat and sensible heat combined) and deviation in equivalent potential temperature of the respective storms. We note that even though there is higher rate of surface fluxes for MRF compared to other experiments throughout the integration period it remains a weak storm at least till 60th h of forecast. We attribute this kind of behavior pattern because of large values of eddy exchange coefficients and deep vertical mixing in MRF scheme. We have considered MY being the best in the group based on combination of factors such as track errors, storm intensity and pattern of intensification rate of the storm.

Finally six more experiments are carried out to investigate sensitivity of microphysical parameterization schemes (MPS) on cyclone intensity and track. We note a moderate impact of microphysics on cyclone forecast tracks obtained from these experiments. However, robust impact of microphysics on storm intensity forecast is evident. Results clearly demonstrate that direct impact of explicit moisture schemes on storm track, intensity, structure and precipitation. In this group the storm produced from WR experiment is intense and somewhat close to the observed IMD estimates. We also note that WR storm reasonably able to replicate the pattern of rapid intensification phase of the storm. We have elucidated two possible mechanisms responsible for this intensification of WR storm. These are absence of large scale melting and evaporation processes from frozen hydrometeors (i.e., reduction in cooling tendency within the core) and less water loading in WR experiment. One of the highlights of the MPS results is the substantial reduction in rain water amount for Sc scheme throughout the forecast duration. Further studies are warranted to elucidate and correct this kind of systematic deficiencies in the Sc microphysical scheme. Here, we would also like to underscore the point that performances of microphysical schemes have a stronger resolution dependency. This set of experiments is carried out at 10-km resolution, which is higher than the previous set of experiments (i.e., CPS and PBL), therefore positive impact of resolution increase to overall skill of the forecast cannot be completely discarded.

In general, we note that model forecast track as well as intensity is more sensitive to cumulus schemes than PBL and explicit moisture schemes. This strongly indicates that choosing appropriate cumulus parameterization scheme in the model will greatly minimize the errors in track forecast. All the intensity forecasts (in all groups) have a tendency to intensify the storm even after 54 forecast hour (observed storm started weaken after 54 h) this is possibly due to slow propagation speed of the storms which keep them over the

ocean throughout the integration phase prohibiting landfall. We do agree that along with model parameterization schemes there are several other factors responsible in a numerical model for an accurate cyclone prediction such as horizontal resolution, coupling with ocean, data assimilation, model initialization. We do understand that one case study might not able to substantially support the findings; however, we strongly feel that findings of this work will definitely supplement the current understanding of cyclone prediction (intensity as well as track). In future, we would like to study the impact of CPS, PBL and microphysics sensitivity for couple of storms with different strengths.

References

Anthes RA (1982) Tropical cyclones: their evolution, structure and effects. Meteorol Monogr Ser, Amer Meteor Soc Boston. 19 41:208–209

Bayers HR (1944) General meteorology. McGraw-Hill, NY, p 645

Betts AK (1986) A new convective adjustment scheme. Part I: observational and theoretical basis. Quart J Roy Meteor Soc 112:677–692

Betts AK, Miller MJ (1986) A new convective adjustment scheme. Part II: single column tests using GATE wave, BOMEX, ATEX, and Arctic air-mass data sets. Quart J Roy Meteor Soc 112:693–709

Betts AK, Simpson J (1987) Thermodynamic budget diagrams for hurricane subcloud layer. J Atmos Sci 44:842–849

Braun SA, Tao W-K (2000) Sensitivity of high resolution simulation of Hurricane Bob (1991) to planetary boundary layer parameterizations. Mon Weather Rev 128:3941–3961

Briegleb B (1992) Delta-Eddington Approximation for Solar Radiation in the NCAR Community Climate Model. J Geophys Res 97(D7):7603–7612

Burk SD, Thompson WT (1989) A vertically nested regional numerical weather prediction model with second-order closure physics. Mon Weather Rev 117:2305–2324

Davis CA, Bosart LF (2001) Numerical simulation of the genesis of hurricane Diana (1984). Part I: control simulation. Mon Weather Rev 129:1859–1881

Davis CA, Bosart LF (2002) Numerical simulation of the genesis of hurricane Diana (1984). Part II: sensitivity of track and intensity prediction. Mon Weather Rev 130:1100–1124

Deardorff JW (1972) Parameterization of the planetary boundary layer for use in general circulation models. Mon Wea Rev 100:93–106

Dudhia J (1989) Numerical study of convection observed during the Winter Monsoon Experiment using a mesoscale two-dimensional model. J Atmos Sci 46:3077–3107

Emanuel KA (1986) An air-sea interaction theory for tropical cyclones. Part I: steady state maintenance. J Atmos Sci 43:585–604

Emanuel KA, Raymond DJ (eds.) (1993) The representation of cumulus convection in numerical models. Meteorol Monogr Ser, Am Meteorol Soc, Boston, MA 46, p 246

Frank WM (1983) The cumulus parameterization problem. Mon Wea Rev 111:1859–1871

Grell GA (1993) Prognostic evaluation of assumptions used by cumulus parameterizations. Mon Wea Rev 121:764–787

Grell GA, Dudhia J, Stauffer DR (1994) A description of the fifth-generation Penn State/NCAR mesoscale model (MM5). NCAR Technical Note, NCAR/TN-398 + STR, p 117

Hong SY, Pan HL (1996) Nocturnal boundary layer vertical diffusion in a medium-range forecast model. Mon Weather Rev 124:2322–2339

India Meteorology Department (2008) Report on Cyclonic disturbances over North Indian Ocean during 2007, RSMC-Tropical Cyclones, IMD, New Delhi, pp. 30–37

Kain JS (2004) The Kain-Fritsch convective parameterization: an update. J Appl Meteor 43:170–181

Kain JS, Fritsch JM (1993) Convective parameterization for mesoscale models: the Kain-Fritsch scheme. The representation of cumulus convection in numerical models. Meteorol Monogr Amer Met Soc 46:165–170

Kessler E (1969) On the distribution and continuity of water substance in atmospheric circulations. Meteor Monogr 10, No. 32, Am Meteor Soc, p 84

Kiehl JT, Hack JJ, Briegleb BP (1994) The simulated earth radiation budget of the NCAR CCM2 and comparison with the earth radiation budget experiment. J Geophys Res 99:20815–20827

Kuo HL (1965) On formation and intensification of tropical cyclones through latent heat release by cumulus convection. J Atmos Sci 22:40–63

Kuo YH, Bresch JF, Cheng MD, Kain J, Parsons DB, Tao W-K, Zhang DH (1997) Summary of a mini workshop on cumulus parameterization for mesoscale models. Bull Amer Met Soc 78:475–491

Liu Y, Chen F, Warner T, Swerdlin S, Bowers J, and Halvorson S (2004) Improvements to surface flux computations in a non-local-mixing PBL scheme, and refinements on urban processes in the Noah land-surface model with the NCAR/ATEC real-time FDDA and forecast system. 20th Conference on Weather Analysis and Forecasting/16th Conference on Numerical Weather Prediction. 11–15 January, 2004, Seattle, Washington

Lord SJ, Willoughby HW, Piotrowicz JM (1984) Role of a parameterized ice-phase microphysics in an axisymmetric tropical cyclone model. J Atmos Sci 41:2836–2848

Mandal M, Mohanty UC (2006) Numerical experiments for improvement in mesoscale simulation of Orissa super cyclone. Mausam 57:79–96

Mandal M, Mohanty UC, Raman S (2004) A study on the impact of parameterization of the physical processes on prediction of tropical cyclones over the Bay of Bengal with NCAR/PSU mesoscale model. Nat Hazards 31:391–414

Mellor GL, Yamada T (1982) Development of a turbulence closure model for geophysical fluid problems. Rev Geophys Space Phys 20:851–875

Molinari J, Dudek M (1992) Parameterization of convective precipitation in mesoscale numerical models: a critical review. Mon Weather Rev 120:326–344

Ooyama K (1969) Numerical simulation of the life cycle of the tropical cyclone. J Atmos. Sc 26:3–40

Palmén E, Riehl H (1957) Budget of angular momentum and energy in tropical cyclones. J Meteor 14: 150–159

Pattnaik S, Krishnamurti TN (2007) Impact of cloud microphysical processes on hurricane intensity, part 2: sensitivity experiments. Meteorol Atmos Physics 97:127–147

Prater BE, Evans JL (2002) Sensitivity of modeled tropical cyclone track and structure of hurricane Irene (1999) to the convective parameterization scheme. Meteorol Atmos Phys 80:103–115

Puri K, Miller MJ (1990) Sensitivity of ECMWF analysis forecast of tropical cyclones to cumulus parameterization. Mon Weather Rev 118:1709–1741

Rao DVB, Prasad DH (2006) Numerical prediction of Orissa super cyclone (1999): sensitivity to the parameterization of convection, boundary layer and explicit moisture processes. Mausam 57:61–78

Rao DVB, Prasad DH (2007) Sensitivity of tropical cyclone intensification to boundary layer and convective processes. Nat Hazards 41:429–445

Reisner J, Rasmussen RJ, Bruintjes RT (1998) Explicit forecasting of supercooled liquid water in winter storms using the MM5 mesoscale model. Quart J R Met Soc 124B:1071–1107

Riehl H (1954) Tropical meteorology. McGraw-Hill, NY, p 392

Rotunno R, Emanuel KA (1987) An air–sea interaction theory for tropical cyclones. Part II: evolutionary study using a nonhydrostatic axisymmetric numerical model. J Atmos Sci 44:542–561

Schultz P (1995) An explicit cloud physics parameterization for operational numerical weather prediction. Mon Weather Rev 123:3331–3343

Srinivas CVR, Venkatesan DV, Rao DVB, Prasad DH (2007) Numerical simulation of Andhra Severe Cyclone (2003): model sensitivity to the boundary layer and convection parameterization. Pure Appl Geophys 164:1465–1487

Tao WK, Simpson J (1993) The Goddard cumulus ensemble model. Part I: model description. Terr Atmos Ocean Sci 4:35–72

Thompson G, Rasmussen RM, Manning K (2004) Explicit forecast of winter precipitation using an improved bulk microphysics scheme: part I: description and sensitivity analysis. Mon Weather Rev 132:519–542

Trivedi DK, Mukhopadhyay P, Vaidya SS (2006) Impact of physical parameterization schemes on the numerical simulation of Orissa super cyclone. Mausam 57:97–110

Wang Y (2002) An explicit simulation of tropical cyclones with a triply nested movable mesh primitive equation model: TCM3. Part II: model refinements and sensitivity to cloud microphysics parameterization. Mon Weather Rev 130:3022–3036

Willoughby HE, Jin H-L, Lord SJ, Piotrowicz JM (1984) Hurricane structure and evolution as simulated by an axisymmetric nonhydrostatic numerical model. J Atmos Sci 41:1568–1589

Yang MJ, Ching L (2005) A modeling study of Typhoon Toraji (2001): physical parameterization sensitivity and topographic effect. Terr Atmos Oceanic Sci 16:177–213

Zhang DL, Kain JS, Fritsch JM, Gao K (1994) Comments on "Parameterization of convective precipitation in mesoscale numerical models: a critical review". Mon Weather Rev 122:2222–2231